Conformational State of the SecYEG-Bound SecA Probed by Single Tryptophan Fluorescence Spectroscopy†

Paolo Natale, Tanneke den Blaauwen,‡ Chris van der Does,§ and Arnold J. M. Driessen*

Department of Molecular Microbiology, Groningen Biomolecular Sciences and Biotechnology Institute, University of Groningen, 9750 AA Haren, The Netherlands

Received November 30, 2004; Revised Manuscript Received March 11, 2005

ABSTRACT: The SecYEG complex is a membrane-embedded channel that permits the passage of precursor proteins (preproteins) across the inner membrane of *Escherichia coli.* SecA is a molecular motor that associates with the SecYEG pore and drives the stepwise translocation of preproteins across the membrane through multiple cycles of ATP binding and hydrolysis. We have investigated the conformational state of soluble and SecYEG-bound SecA using single tryptophan mutants of SecA. The fluorescence spectral properties of the single tryptophans of SecA and their accessibility to the quencher acrylamide demonstrate that SecA undergoes a conformational change that results in a more compact structure upon binding of ATP and binding to the SecYEG pore. In addition, SecYEG-bound SecA undergoes ATP-dependent conformational changes that are not observed for soluble SecA. These data support a model in which binding to the SecYEG channel has a major impact on the SecA conformation.

SecA is a membrane-associated ATPase that drives the transport of precursor proteins (preproteins) across the bacterial cytoplasmic membrane (*1*−*3*). SecA binds with high affinity to the SecYEG complex (*1*, *4*, *5*), which constitutes the pore across the membrane that allows the transport of unfolded preproteins across the membrane as well as the integration of membrane proteins into the lipid bilayer (*6*−*9*). SecA and SecYEG together form the preprotein *translocase.* Binding and hydrolysis of ATP by SecA is essential for preprotein translocation. It allows the cycling of SecA between a membrane-bound and free cytosolic form (*5*, *10*) and simultaneously the binding and release of the preprotein by SecA. Consecutive rounds of ATP binding and hydrolysis result in the stepwise translocation of the preprotein across the membrane (*11*, *12*).

Recently, the crystal structures of dimeric (*13*) and monomeric (*14*) *Bacillus subtilis* and dimeric *Mycobacterium tuberculosis* SecA (*15*) were solved at atomic resolution. Superposition of the three structures showed a similar domain organization and overall folds (*15*). On the basis of biochemical and structural evidence (*10*, *12*, *16*−*21*), functions have been assigned to the different domains of SecA (See Figure 1). A high-affinity nucleotide-binding site is located in the first nucleotide-binding fold (Figure 1, NBF-I[1] in violet). Mutations that impair binding and hydrolysis of ATP at this site (*17*, *22*) inhibit translocation and result in fractionation of SecA in a membrane-bound form (*10*, *23*). Indeed, release of SecA from SecYEG during or after completion of translocation requires the hydrolysis of ATP (*24*, *25*). This suggests that SecA cycling and preprotein translocation are coupled processes. A low-affinity binding site for nucleotides (*17*, *18*) is located in the second nucleotide-binding fold (NBF-II, light blue). Hydrolysis of ATP at this site has also been suggested to loosen the SecA structure to facilitate nucleotide release from NBF-I (*13*, *26*). However, other evidence indicates that this ATP-binding site is nonfunctional (*21*, *27*) and that NBF-II fulfils a regulatory function (intramolecular regulator of ATP hydrolysis, IRA2) (*28*). The NBF-II of *Escherichia coli* SecA contains an additional stretch of 29 amino acids (Gly 517−Ala 548) that is not present in Gram-positive microorganisms (*13*). Other domains identified in SecA (Figure 1) are the preprotein cross-linking domain (PPXD, yellow) (*16*), the α-helical scaffold domain (HSD, dark green), the helical wing domain (HWD, light green), and the carboxyl-terminal linker (CTL, red) (*13*, *15*). The HSD is the only domain that contacts all other subdomains in SecA, and it seems to function as a global template of the SecA structure (*13*, *15*). The N-terminal part of this domain is connected to the NBF-II domain and is involved in packing interactions with NBF-I. The C-terminal part of the HSD domain is connected to the HWD, where it forms the interface of the physiological SecA dimer (*13*) and to the CTL that contains the primary SecB-binding site (*13*, *29*, *30*).

† This work was supported by the Council for Chemical Sciences of The Netherlands Organization for Scientific Research CW-NWO and subsidized by the Dutch Organization for the Advancement of Scientific Research (NWO).

* To whom correspondence should be addressed: Telephone: 31-50-3632164. Fax: 31-50-3632154. E-mail: a.j.m.driessen@rug.nl.

‡ Present address: Molecular Cytology, Swammerdam Institute for Life Sciences, Faculty of Science, University of Amsterdam, The Netherlands.

§ Present address: Institute of Biochemistry, Biocenter, Goethe-Universität Frankfurt, Germany.

[1] Abbreviations: IPTG, isopropyl-*β*-D-thiogalactopyranoside; DOPE, 1,2-dioleoyl-*sn*-glycero-3-phosphoethanolamine; DOPG, 1,2-dioleoyl-*sn*-glycero-3-phosphoglycerol; HSD, helical scaffold domain; HWD, helical wing domain; NBD, nucleotide-binding domain; NBF, nucleotide-binding fold; PPXD, precursor protein cross-linking domain; SSD, substrate-specific domain; Trp, tryptophan.

10.1021/bi047488r CCC: $30.25
Published on Web 04/09/2005

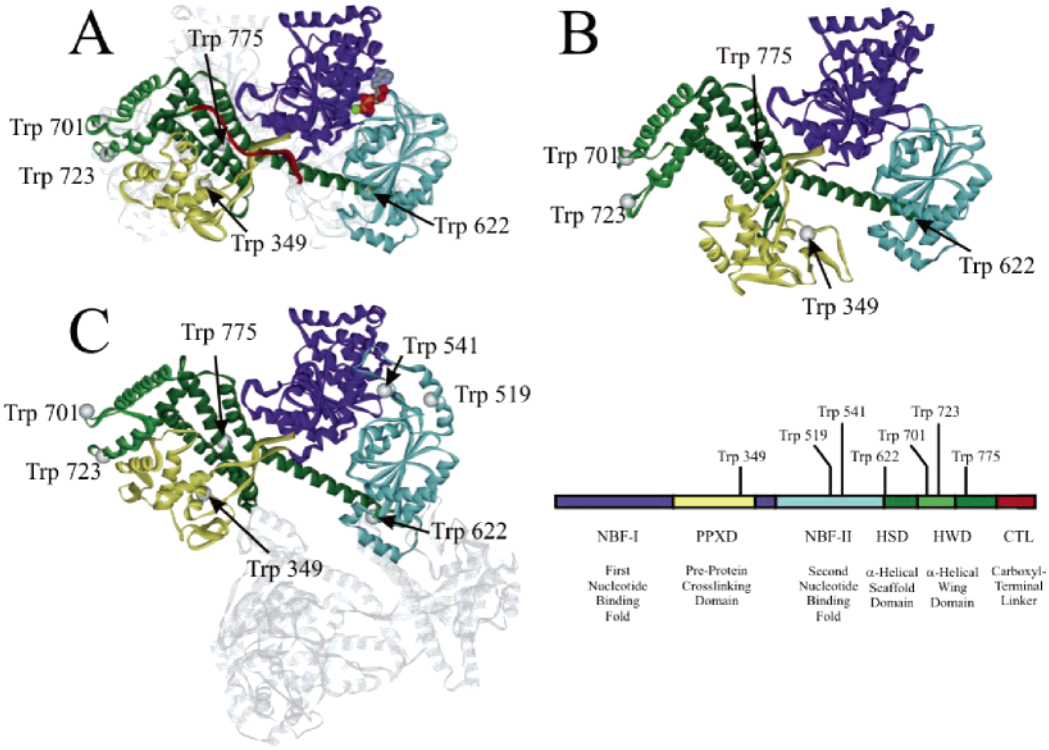

FIGURE 1: Localization of tryptophan residues in the *E. coli* SecA structure. The structure of *E. coli* SecA was modeled on basis of the crystal structure of (A) *B. subtilis* dimeric SecA (*13*), (B) *B. subtilis* monomeric SecA (*14*), and (C) *M. tuberculosis* SecA (*15*) using the Swiss-Model module of SwissPDBViewer 3.7 (*53*). The different domains are indicated in color (NBF-I, violet; PPXD, yellow; NBF-II, light blue; HSD, dark green, HWD, light green; CTL, red). For the dimeric SecA structures (A and C), the second protomer is represented as a gray ribbon. The endogenous tryptophan residues are shown as gray spheres. The ADP molecule present in A indicates the position of the nucleotide when bound to SecA. The nucleotide is omitted in B and C for simplification.

Recently, the crystal structure of the archaeon *Methanococcus jannaschii* Sec61 complex was solved (*31*). This complex is approximately 50% homologous to the *E. coli* SecYEG protein complex. A comparison of the crystal structure with an electron-density map of 2D crystals of the *E. coli* SecYEG complex (*32*) showed a similar arrangement of the transmembrane segments (*31*). It has been suggested that the Sec61 complex forms an "hourglass" shaped water-filled channel with a ring of hydrophobic residues at its constriction. This putative channel is closed on the periplasmic face of the membrane by a plug-like structure formed by a re-entrance loop that connects transmembrane segments 1 and 2 of Sec61α (*9*, *31*). Because archaea lack a SecA homologue, it is difficult to access the binding site for SecA from the structure of the Sec61 complex. Moreover, the precise interactions between SecA, SecYEG, and the preprotein and even the stoichiometry of these interactions are presently a matter of debate (*32*−*37*).

The mechanism of SecA-mediated protein translocation is complex and likely requires nucleotide-induced structural rearrangements of SecA engaged with the SecYEG complex and a preprotein substrate (*1*, *10*, *11*, *38*). Surprisingly, both in the *B. subtilis* and *M. tuberculosis* SecA structures, only small structural differences were observed when the apo and different nucleotide-bound holo forms were compared (*13*, *15*). Large conformational differences can be observed when comparing the dimeric (*13*) and monomeric (*14*) *B. subtilis* SecA structures. In the monomeric structure, a deep groove is exposed and it has been suggested that this region interacts with the substrate polypeptides (*14*). However, this large change in conformation is not nucleotide-dependent and seems unique for the monomeric crystal form. Currently, it is not understood how the energy of ATP binding and hydrolysis is utilized for preprotein translocation. Moreover, to understand the mechanism of motor action, it will be necessary to investigate the structure and function of SecA while it is functionally associated with the SecYEG complex.

Here, we have used fluorescence spectroscopy to investigate the conformational state of the SecYEG-bound SecA protein. *E. coli* SecA contains seven endogenous tryptophan residues, i.e., at positions 349, 519, 541, 622, 701, 723, and 775 (*39*). The primary amino acid sequences of *B. subtilis* and *M. tuberculosis* SecA show about 50% similarity to the *E. coli* SecA, and modeling of the *E. coli* SecA on the published crystal structures (*13*−*15*) enabled us to position the endogenous tryptophan residues in the different domains of SecA (gray spheres in Figure 1). Trp 349 is located within the PPXD. Trp 519 and Trp 541 are located in the Gram-negative-specific insertion region within NBF-II (*13*). This insertion region faces the interface with NBF-I, where the nucleotide binds (Figure 1A). Trp 622 is located at the transition of NBF-II and the HSD. Trp 701 and Trp 723 are part of the flexible HWD. Finally, Trp 775 is part of the HSD. The endogenous tryptophan residues cover most of the *E. coli* SecA domains and therefore may provide detailed information on its overall conformational state. In an early stage, total tryptophan fluorescence studies have been performed to monitor the thermal unfolding of soluble *E. coli* SecA to understand the molecular processes associated with nucleotide, preprotein, and membrane binding (*3*, *13*, *26*, *40*−*45*). SecA was found to be destabilized by the nonhydrolysable ATP analogue AMP−PNP (*13*, *40*, *41*),

Table 1: Plasmids Used in This Study

plasmids	description	source or reference
pET104	*Sal*I−*Eco*RV *secA* fragment (970−1323 bp)[a]	*41*
pET105	*Eco*RV−*Kpn*I *secA* fragment (1323−1676 bp)[a]	*41*
pET109	*Kpn*I−*Pst*I *secA* fragment (1323−1676 bp)[a]	*41*
pET110	*Pst*I−*Pst*I *secA* fragment (2120−2595 bp)[a]	*41*
pMKl18	wild type *secA* under control of *lac* promoter	*49*
pET147	Trp 349 *secA* under control of *lac* promoter	this paper
pET115	Trp 519 *secA* under control of *lac* promoter	this paper
pET118	Trp 541 *secA* under control of *lac* promoter	this paper
pET108	Trp 622 *secA* under control of *lac* promoter	this paper
pET175	Trp 701 *secA* under control of *lac* promoter	this paper
pET178	Trp 723 *secA* under control of *lac* promoter	this paper
pET177	Trp 775 *secA* under control of *lac* promoter	this paper
pET170	Trp less *secA* under control of *lac* promoter	this paper

[a] bp starting from ATG start codon of the *secA* gene.

preproteins (*42*), and membranes containing anionic phospholipids (*3*). On the other hand, ADP stabilized the conformation of SecA (*41*). Single tryptophan (Trp 701 and Trp 775) (*41*) and tryptophan substitution (*43*) mutants of soluble *E. coli* SecA suggested that the carboxyl-terminal domain (HSD, HWD, and CTL) of SecA is a very flexible region that undergoes conformational changes upon binding of SecA to nucleotides (*41*), signal peptide, or liposomes (*43*). These conformational changes correspond to the earlier described temperature-induced flexibility of this domain (*2*).

We have exploited the environmental sensitive spectral properties of the single tryptophan mutants and their accessibility for the collisional quencher acrylamide to investigate the conformational state of the SecYEG-bound SecA protein. Our data indicate that binding of SecA to SecYEG results in an altered conformational state of SecA. Strikingly, the SecYEG-bound SecA undergoes ATP-dependent conformational changes that are not observed for the soluble SecA. These data provide structural insight into the mechanism of the SecYEG-induced elevated nucleotide release kinetics at the SecA protein (*38*).

EXPERIMENTAL PROCEDURES

Bacterial Strains and Growth Media. Strains were grown in Luria Bertani (LB) broth or LB agar (*46*) supplemented with 100 μg/mL of ampicillin, 0.5% (w/v) glucose, or 0.5 mM isopropyl-β-D-thiogalactopyranoside (IPTG), as required. Construction of the plasmids was done in *E. coli* JM101 or JM110 (*41, 47*). Complementation of chromosomal *secA* and overexpression using the plasmids bearing the tryptophanless or single tryptophan SecA mutants were done in *E. coli* strain MM66 (*geneX*^{am} and *supF*^{ts}) (*48*).

Construction of the Tryptophanless and Single Tryptophan SecA Mutants. The construction of the tryptophanless SecA was described by den Blaauwen et al. (*41*). Single amino acid substitutions were cloned in pMKL18 (*49*) to create single tryptophan mutants under control of the IPTG-inducible *lac* promoter (Table 1).

Complementation of the Temperature-Sensitive Phenotype of E. coli MM66. Plasmids were transformed into *E. coli* MM66 (*48*) and checked for complementation of the chromosomal *secA* by growth and colony formation on LB agar plates (*46*) supplemented with 100 μg/mL ampicillin, 0.5% w/v glucose, and 0.5 mM IPTG at 30 °C and the nonpermissive temperature of 37 and 42 °C.

Expression and Purification of SecA. E. coli MM66 cells transformed with plasmids containing tryptophanless or single tryptophan *secA* under control of the IPTG-inducible *lac* promoter were grown overnight at 30 °C in LB containing 0.5% glucose and 100 μg/mL ampicillin. Cells were diluted 1000-fold in LB containing 100 μg/mL ampicillin and were grown at 37 °C. SecA expression was induced at an $OD_{660} = 0.6$ with 0.5 mM IPTG. After 2 h, cells were harvested by centrifugation and resuspended in a 50 mM Tris-HCl at pH 7.5 buffer containing 10% (w/v) sucrose. The suspension was frozen in liquid nitrogen and stored at −80 °C. For the purification of SecA, cells were rapidly thawed and subsequently lysed by French press treatment. Membranes and other insoluble material were removed by centrifugation at 125000*g* for 90 min at 4 °C. SecA was purified using Reactive Blue 4 Agarose (Sigma) and HiTrap Q HP Sepharose (Pharmacia) columns as described (*50*). Finally, SecA was concentrated using a Centriprep 50 concentrator (Millipore) and applied on a Superose 12 gel-filtration column (Pharmacia) equilibrated with 50 mM Tris-HCl at pH 7.5 and 1 mM DTT. Purified proteins were analyzed by Coomassie Brilliant Blue stained SDS−PAGE and found to be more than 95% pure. The concentration of wild-type (WT) SecA was determined spectroscopically using a molar extinction coefficient at 280 nm of 83 000 M^{-1} cm^{-1} for monomeric SecA. Comparative SDS−PAGE with WT SecA as a reference was used to estimate the protein concentrations of the single tryptophan mutants.

Steady-State Fluorescence Measurements. Tryptophan emission spectra were collected on a temperature-controlled SLM-Aminco 4800C spectrofluorometer (SLM-Aminco, Urbana, IL) with Glan-Thompson polarizers. The slit widths for the excitation and emission beam were set open, and the excitation and emission polarizer were set to 90° and 0°, respectively, to reduce light scatter. Tryptophan emission spectra from 320 to 450 nm were scanned at a rate of 1 nm/s using an excitation wavelength of 295 nm. Fluorescence spectra were corrected by substacting the buffer or a control containing the tryptophanless SecYEG proteoliposomes for the measurements with the soluble SecA and SecYEG-bound SecA, respectively (*38*).

Tryptophan Fluorescence Quenching of Single Tryptophan SecA Mutants. Small aliquots of a 1 M acrylamide solution prepared in the protein buffer (50 mM KCl, 50 mM Tris-HCl at pH 7.5, and 5 mM $MgCl_2$) were added in a microquartz cuvette to a 120 μL volume containing 0.14 μM soluble SecA or 0.07 μM SecYEG-bound SecA (*38*). When indicated, 1.6 mM ATP was added. All measurements were repeated 3 times, and the data were corrected for dilution effects and analyzed using the Stern−Volmer equation (eq 1) (*51*).

$$F_0/F = 1 + K_{SV}[Q] \quad K_{SV} = k_q\tau_0 \tag{1}$$

where F_0 and F are the fluorescence intensities in the absence and presence of the quencher, respectively, $[Q]$ is the concentration of the quencher, and K_{SV} is the Stern−Volmer constant. K_{SV} can be considered a reliable measure of the bimolecular collisional constant for quenching of the tryptophan because $K_{SV} = k_q\tau_o$, where k_q is the bimolecular collisional constant and τ_0 is the lifetime constant of the fluorophore in the absence of the quencher (*51*). Assuming

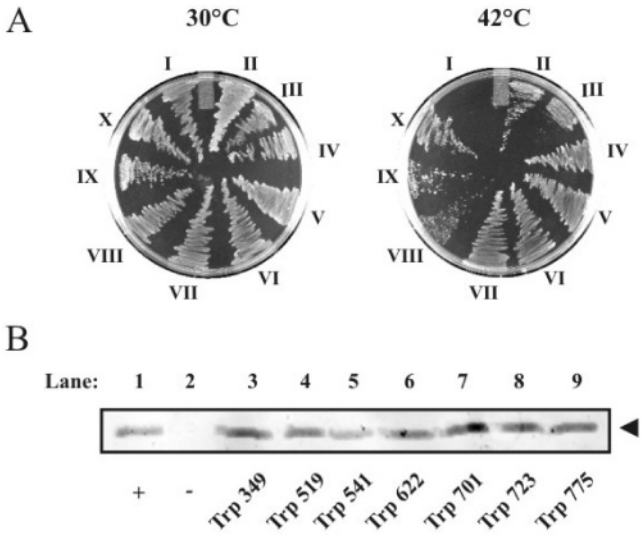

FIGURE 2: Activity of tryptophanless and single tryptophan SecA mutants. (A) Complementation of the temperature-sensitive phenotype of *E. coli* MM66 (*48*). Growth of *E. coli* MM66 transformed with an empty vector (pUC19, I), tryptophanless SecA (II), WT SecA (III), and plasmids overexpressing single tryptophan mutants (Trp 349, IV), (Trp 519, V), (Trp 541, VI), (Trp 622, VII), (Trp 701, VIII), (Trp 723, IX), and (Trp 775, X). (B) *In vitro* protein translocation of proOmpA. Lane 1, WT SecA (positive control); lane 2, WT SecA without ATP (negative control); lanes 3−9, single tryptophan SecA mutants as indicated. The arrow indicates the protease-protected proOmpA.

that the lifetime τ_0 is not changed after nucleotide or SecYEG binding, K_{SV} reflects the change in accessibility of the tryptophan residue to the quencher. When the fluorescence quenching F is more than 50% of the starting fluorescence intensity F_0, the data can deviate from the linearity and are considered unreliable (*51*). Quenching was linear up to 40 mM acrylamide, and Stern−Volmer constants were calculated from the data obtained in this linear range.

Other Methods. In vitro translocation of proOmpA into tryptophanless SecYEG proteoliposomes was performed as described (*52*). *E. coli* SecA (*39*) was modeled on the published crystal structures of *B. subtilis* SecA (1M6N and 1M74) (*13*), (1TF5 and 1TF2) (*14*), and *M. tuberculosis* SecA (1NKT and 1NL3) (*15*) using the Swiss-Model module of Swiss-PDB Viewer 3.7 (*53*).

RESULTS

Functional Complementation of the E. coli MM66 Temperature-Sensitive Strain by Single Tryptophan SecA Mutants. SecA contains seven endogenous tryptophan residues at positions 349, 519, 541, 622, 701, 723, and 775 (*39*). We have previously described the construction of tryptophanless and single tryptophan SecA by replacement of the endogenous tryptophans by phenylalanines (*41*). The genes encoding tryptophanless and the single tryptophan mutants of *secA* were cloned under control of the IPTG-inducible *lac* promoter (*49*) (Table 1). *E. coli* MM66 contains an amber mutation in *geneX* and a temperature-sensitive suppressor tRNA and is unable to grow at 37 and 42 °C because of the lack of SecA expression (*48*). The tryptophanless and single tryptophan mutants of SecA were expressed in *E. coli* MM66. At 30 °C, the permissive temperature, all transformants showed normal growth on the plate (Figure 2A). At 37 (data not shown) and 42 °C, the cells expressing the chromosomal *secA* showed no colony formation (Figure 2A, I). In contrast, the plasmid encoded WT and tryptophanless and single tryptophan mutants restored growth (Figure 2A, II−X), demonstrating that these mutants of SecA are functional. The tryptophanless mutant was only used as a template for the construction of the single tryptophan mutants and was not further employed in this study.

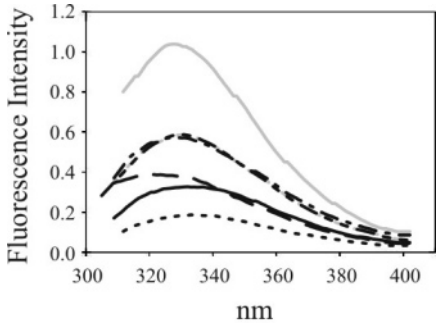

FIGURE 3: Tryptophan emission spectra of single tryptophan SecA mutants. Trp 349 (—), Trp 519 (•••), Trp 541 (- - -), Trp 622 (— - -), Trp 701 (gray — —), Trp 723 (—•) and Trp 775 (gray —). The concentration of SecA was 0.14 μM.

In Vitro Translocation Activity of Single Tryptophan SecA Mutants. All single tryptophan mutants of SecA were overexpressed in *E. coli* MM66 (*48*) and purified to homogeneity. The purified SecA mutant proteins were tested for *in vitro* translocation of proOmpA into proteoliposomes reconstituted with the tryptophanless SecYEG complex (*38*). With all single tryptophan SecA proteins, translocation of proOmpA could be demonstrated (Figure 2B). SecA (Trp 541) was about half as active as the WT SecA. Because all single tryptophan mutants were active, they could be used as reporters for the conformational states of SecA.

Spectral Characteristics of the Soluble and SecYEG-Bound Single Tryptophan SecA Mutants. The tryptophan emission spectra of the individual single tryptophan mutants of SecA were recorded. Samples were excited at 295 nm to minimize the contribution of tyrosine to the fluorescence signal (*51*). As observed previously, the C-terminal tryptophan residues Trp 701, Trp 723, and Trp 775 showed a major contribution to the total SecA protein fluorescence signal (*43*) (Figure 3). In addition, we observed a significant contribution of Trp 622 to the total fluorescence signal. All other single tryptophan SecA mutants (Trp 349, Trp 519, and Trp 541) showed clear but lowered emission spectra.

To investigate the molecular environment of the different tryptophan residues, emission spectra of the soluble and SecYEG-bound SecA mutants were recorded both in the absence and presence of ATP. For this purpose, SecA proteins were incubated with proteoliposomes reconstituted with the tryptophanless SecYEG complex, whereupon the SecYEG-bound fraction was collected by centrifugation through a glycerol cushion as described previously (*38*). The recorded tryptophan emission spectrum provides information about the local environment of the individual tryptophan residues, wherein the emission maximum (λ_{max}) at a shorter or longer wavelength is indicative for a hydrophobic or hydrophilic environment, respectively (*51*, *54*). Spectra were recorded before and after the addition of ATP. Because ATP is rapidly hydrolyzed such that only ADP is recovered with SecA (*38*), the obtained data reflect the ADP-bound con-

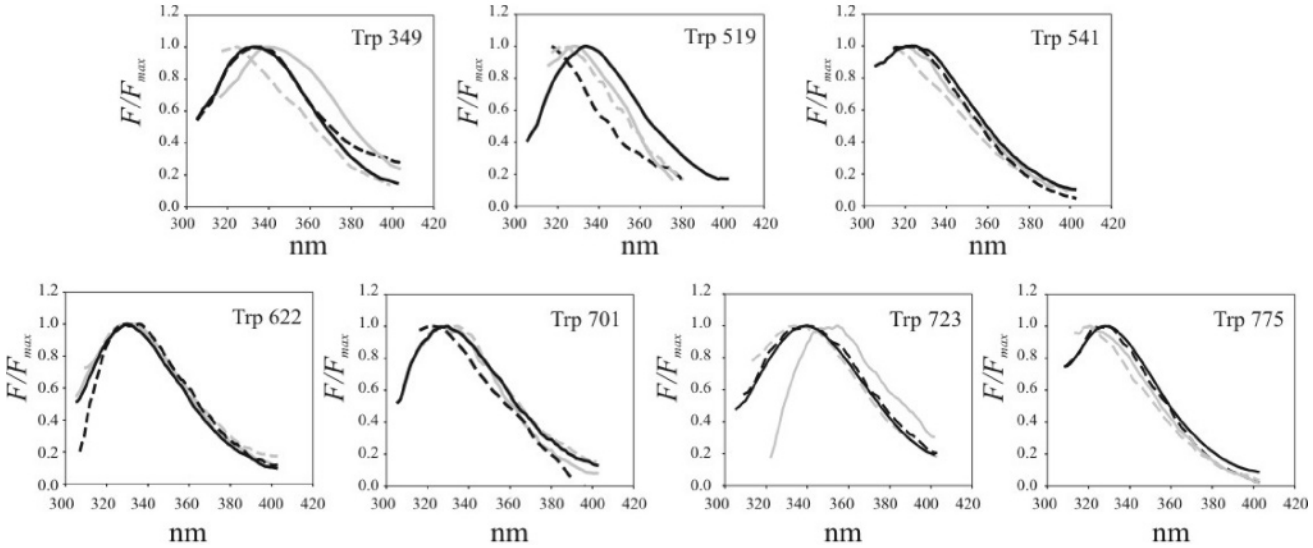

FIGURE 4: Tryptophan emission shifts (λ_{max}) of the single tryptophan SecA mutants. Soluble SecA (black lines) and SecYEG-bound SecA (gray lines) with (- - -) and without (—) ATP. The spectra are normalized by dividing the fluorescence intensity (F) by the fluorescence maximum (F_{max}). The fluorescence emission maxima (λ_{max}) are listed in Table 2. The concentration of soluble and SecYEG-bound SecA was 0.14 and 0.07 μM, respectively.

Table 2: Emission Maximum of Tryptophan Fluorescence of Single Tryptophan SecA Mutants[a]

		Trp fluorescence maximum (nm)						
		Trp 349	Trp 519	Trp 541	Trp 622	Trp 701	Trp 723	Trp 775
SecA	−ATP	332	335	324	330	329	339	328
	+ATP	336	317	323	332	320	340	330
SecYEG-bound SecA	−ATP	339	327	320	336	327	355	321
	+ATP	326	322	315	335	335	334	320

[a] Excitation at 295 nm. Values shown have an error of the mean of ±3.6 nm.

formation of SecA. The positions of λ_{max} for the different tryptophan SecA mutants in the soluble and SecYEG-bound state are summarized in Table 2. Several changes in the λ_{max} of single tryptophans of SecA are observed upon binding to the SecYEG complex, whereas others (e.g., Trp 622) are completely invariant (Figure 4). We have classified these λ_{max} changes into minor (between 2 and 3 times the error of the mean of the measurement, 8−12 nm) and major (more than 3 times, >12 nm) shifts.

Binding of SecA to SecYEG results in a minor blue shift of λ_{max} of Trp 519 and a major red shift of Trp 723. This observation suggests that under these conditions Trp 519 enters a more hydrophobic and Trp 723 enters a more hydrophilic environment. These changes in λ_{max} suggest that these sites and their corresponding domains (NBF-II and HWD) either interact directly with SecYEG or that a global conformational rearrangement of SecA upon binding SecYEG also changes the environment of these tryptophan residues and their corresponding domains. The importance of these sites is also apparent after addition of ATP to soluble SecA and SecYEG-bound SecA. For soluble SecA, ATP binding results in a major blue shift of λ_{max} of Trp 519 and a minor blue shift of Trp 701. On the other hand, addition of ATP to the SecYEG-bound SecA caused major blue shifts of Trp 349 and Trp 723 and a minor red shift of Trp 701. In both cases, spectral shifts occur in the HWD (Trp 701 and Trp 723). The change of the molecular environment of Trp 519 (NBF-II) in the presence of ATP as observed for the soluble SecA is smaller for the SecYEG-bound SecA. A large environmental shift of Trp 349 (PPXD) upon ATP addition, which is absent for the soluble SecA, is visible for the SecYEG-bound SecA. The shifts of the tryptophan emission spectra for different tryptophan residues upon ATP and/or SecYEG binding suggest a structural rearrangement of SecA after binding to SecYEG.

SecYEG Binding Changes the Acrylamide Accessibility of Single Tryptophan SecA Mutants. Acrylamide is an uncharged quencher that is often used to determine the solvent accessibility of the tryptophan residues in proteins. Up to a concentration of 60 mM, acrylamide had no effect on the SecA translocation ATPase activity and the *in vitro* protein translocation activity (data not shown). Thus, this quencher can be used to examine the accessibility of the tryptophans of SecA in its different functional states. The acrylamide quenching of the single tryptophan SecA mutants was determined for both free and SecYEG-bound SecA in the presence and absence of ATP. Quenching data were analyzed by Stern−Volmer plots (Figure 5), and the corresponding Stern−Volmer constants (K_{SV}) were calculated (Table 3) (*51*). The high K_{SV} values are consistent with a very loose and open conformation of soluble SecA, as previously suggested (*26*). In general, the addition of ATP results in a 10−40% reduction of acrylamide accessibility, suggesting a more compact conformation, reminiscent of the ADP-bound SecA (*41*). Especially, the accessibility of Trp 519 (● versus ○) was reduced by ~80% upon ATP binding. Together with the major blue shift of λ_{max} of this residue, it appears that it becomes less mobile and/or moves to a more hydrophobic environment upon ATP binding. Binding of SecA to the SecYEG complex renders all tryptophan residues

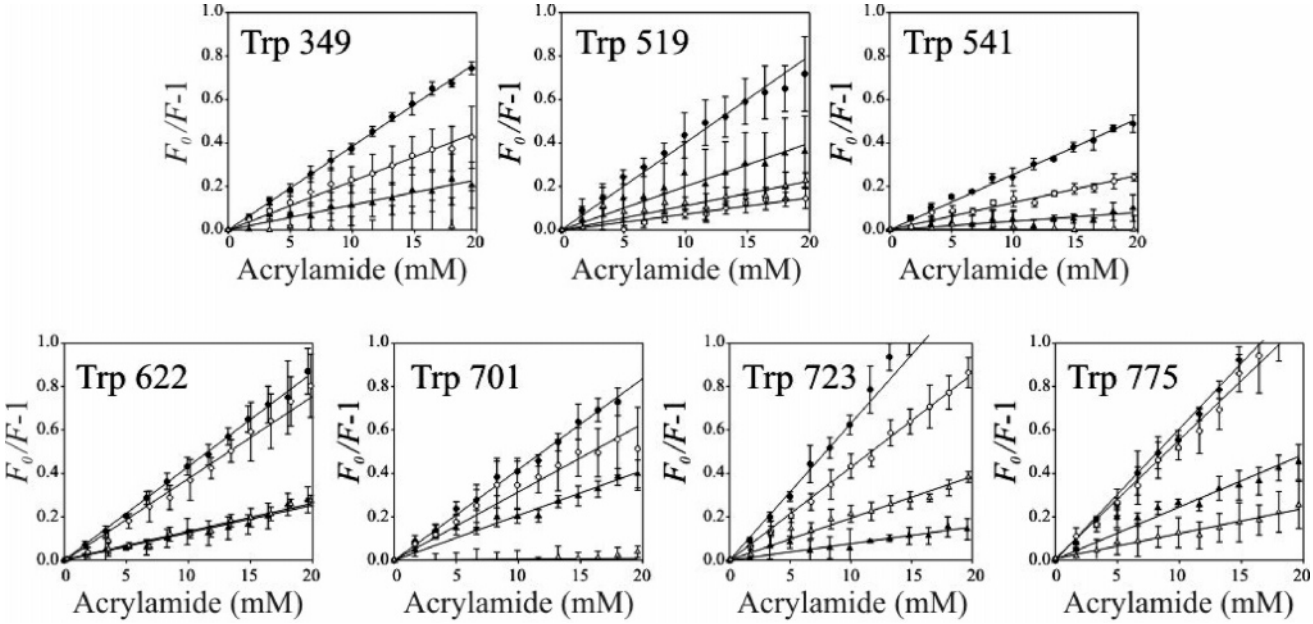

FIGURE 5: Acrylamide accessibility of single tryptophan SecA mutants. Stern−Volmer plots for the acrylamide quenching of the single Trp SecA mutants. Soluble SecA with (○) and without (●) ATP, SecYEG-bound SecA with (△) and without (▲) ATP. Conditions were as described under Figure 4. The slope of each curve provides the Stern−Volmer constants K_{SV}. The K_{SV} values are listed in Table 3.

Table 3: Stern−Volmer Constants of the Acrylamide Accessibility of Single Tryptophan SecA Mutants

		K_{SV} (M^{-1})						
		Trp 349	Trp 519	Trp 541	Trp 622	Trp 701	Trp 723	Trp 775
SecA	−ATP	38.6 ± 0.3	39.1 ± 0.8	25.6 ± 0.3	43.3 ± 0.3	41.8 ± 0.5	71.8 ± 1.2	62.5 ± 1.0
	+ATP	24.7 ± 1.0	7.5 ± 0.5	21.1 ± 0.2	38.7 ± 0.7	31.4 ± 1.1	42.9 ± 0.3	54.7 ± 0.8
SecYEG-bound SecA	−ATP	11.9 ± 0.4	20.3 ± 0.6	4.4 ± 0.3	13.0 ± 0.5	21.0 ± 0.3	8.0 ± 0.4	31.5 ± 0.6
	+ATP	0.1 ± 1.3	11.7 ± 0.3	0.15 ± 0.4	13.3 ± 0.5	0.8 ± 0.9	19.6 ± 0.3	11.9 ± 0.3

at least 2-fold less accessible to acrylamide quenching (Table 3), demonstrating the conversion of a loose soluble SecA conformation into a more compact conformation in the SecYEG-bound state. Trp 723 and Trp 541 become ~80% less accessible to acrylamide in the SecYEG-bound state (▲ versus △ in Figure 5 and Table 3). Unexpectedly, while the accessibility of Trp 723 to externally added quencher is strongly reduced upon SecYEG binding, the major red shift of λ_{max} indicates that this residue increases mobility or moves to a more hydrophilic environment upon ATP binding. This may mean that Trp 723 becomes shielded for acrylamide quenching upon SecYEG binding. Addition of ATP to the SecYEG-bound SecA further reduces the acrylamide accessibility of a number of tryptophan residues (▲ versus △ in Figure 5). Strikingly, Trp 349, Trp 541, and Trp 701 become nearly completely inaccessible. In contrast, Trp 622 remains essentially unchanged, while the accessibility of Trp 723 increases. When these data are taken together, they demonstrate that the binding of SecA to the SecYEG complex and subsequent ATP binding/hydrolysis result in major changes in the acrylamide accessibility of the tryptophan residues. These data are indicative for an unique SecYEG- and ATP-dependent conformational change of SecA.

DISCUSSION

We have investigated the structural properties of soluble and SecYEG-bound SecA by means of site-specific tryptophan fluorescence spectroscopy. *E. coli* SecA contains seven tryptophan residues that are located in distinct domains, such as the PPXD (Trp 349), NBF-II (Trp 519 and Trp 541), at the transition between NBF-II and the HSD (Trp 622), the HWD (Trp 701 and Trp 723), and in the carboxyl-terminal part of the HSD (Trp 775) (*13*, *15*, *39*) (Figure 1). Recently, we have shown that binding of SecA to SecYEG results in a major acceleration of the nucleotide exchange rate at NBF-I in conjunction with a decreased nucleotide-binding affinity (*38*). This implies that there must be a unique conformation of SecA while bound to SecYEG. Here, we have used the fluorescence characteristics and the acrylamide accessibility of single tryptophan mutants of SecA in the soluble and the SecYEG-bound state to examine the structural changes induced by SecYEG binding in the presence and absence of ATP. In our acrylamide accessibility experiments of soluble SecA, high K_{SV} values for some of the single tryptophan mutants were obtained (Table 3). The K_{SV} value for acrylamide quenching of the single exposed Trp residue of SecB is 25 M^{-1}, whereas free tryptophan in buffer or ethanol shows K_{SV} values of 10 and 31 M^{-1}, respectively (unpublished data). When these results are taken together, they imply a very loose conformation of soluble SecA as suggested before (*26*), possibly a molten globular state.

Upon ATP binding, large changes were observed in the fluorescence emission maxima (λ_{max}) of Trp 519 and Trp 701, suggesting that these residues move to a more hydrophobic environment. Reduced acrylamide accessibility was observed for a number of tryptophan residues (10−40%),

but in particular for Trp 519 (~80%). Because ATP is rapidly hydrolyzed by SecA (*38*), these data confirm the more compact shape for the ADP-bound SecA (*41*). This compact shape of SecA is destabilized by different ligands among which are AMP−PNP (*13*, *40*, *41*), preprotein (*42*), and membranes containing anionic phospholipids (*3*).

Upon SecYEG binding, most tryptophan residues and in particular Trp 541 and Trp 723 become less accessible. This suggests that the SecYEG-bound SecA adopts an even more compact state as compared to the ADP-bound soluble SecA. SecYEG binding shifts Trp 349 and Trp 723 to a more hydrophilic environment (red shift of λ_{max}), while Trp 519 and Trp 775 shift to a more hydrophobic environment (blue shift of λ_{max}). The exact sites of interactions of SecA with SecYEG are unknown, but the SecYEG-binding determinants have been localized to the amino-terminal region of SecA (amino acids 1−664) (*20*). This domain can function as an independent ATPase in nucleotide, preprotein, and SecYEG binding (*21*, *28*). In right-side-out vesicles, accessibility studies using the membrane impermeable sulfhydryl-labeling reagent biotin-maleimide (N^{α}-3-maleimidylpropionyl biocytin) identified the accessibility of the single cysteine SecA mutants in the PPXD (Cys 300 and Cys 350), NBF-II (Cys 530), and the CTL (Cys 858 and Cys 896) (*55*). Our acrylamide accessibility data of the SecYEG-bound SecA confirms an interaction of the NBF-II and the HWD, which both undergo packing interactions with the CTL (*13*). Major regions of SecA become highly inaccessible to the quencher when bound to SecYEG, indicating a tight interaction (*56*, *57*).

ATP binding to soluble SecA affects the λ_{max} of Trp 519 and to a lesser extent than the λ_{max} of Trp 701, whereas the ATP binding to the SecYEG-bound SecA shows λ_{max} changes of several tryptophan residues as a major λ_{max} blue shift of Trp 349 and Trp 723 and a minor λ_{max} red shift of Trp 701. The acrylamide accessibility of Trp 349, Trp 541, and Trp 701 was almost completely abolished, while that of Trp 519 and Trp 775 was reduced and that of Trp 723 was increased. Remarkably, Trp 701 moves to a more hydrophilic environment (red shift of λ_{max}) where it is less accessible to acrylamide, while the opposite effect is observed for Trp 723 (blue shift of λ_{max}). The reduced acrylamide accessibility of Trp 723 in the absence of ATP and Trp 701 in the presence of ATP suggest that binding to SecYEG shields the tryptophan residue from the quencher and positions it in a hydrophilic environment like for instance the water-filled channel inside SecYEG (*31*) or SecA (*34*). It should be emphasized that under the conditions employed the bound ATP is immediately hydrolyzed to ADP (*38*). Indeed, preliminary evidence indicates that ADP and ATP induce similar responses with SecA Trp 701 (unpublished data). A study on the differential responses of nonhydrolysable ATP analogues and effects of the precursor protein will be subjects of further investigation.

Ideally, for single tryptophan quenching analysis, the tryptophan residues should be present at the regions and domains that undergo large conformation changes, e.g., an interface between two domains. This study was limited to the positions of the endogenous tryptophan positions. However, three of these positions, Trp 349, Trp 519, and Trp 775 are located on such domain interfaces (Figure 1). Trp 519 is located on the interface between NBF-I and NBF-II. This region is most sensitive to ATP binding in soluble SecA. For soluble SecA, the accessibility of this position is strongly reduced and the λ_{max} is shifted to a more hydrophobic environment. This phenomenon is less obvious in the SecYEG-bound state.

Trp 349 and Trp 775 are part of the PPXD and HSD regions, respectively, and are located on the interface between these two domains (*13*). These domains are connected via large aromatic (Trp 775, Phe 811, and Tyr 803) and charged (Glu 806 and Arg 792) residues (*13*, *28*). The disturbance of this interface weakens the interaction between the C and N domains and causes an elevated ATPase activity (*28*). The open SecA conformation of a monomeric protein (Figure 1B) (*14*) shows a ~60° rigid body rotation of the PPXD domain and the opening of a large groove between the PPXD and HWD disturbing the PPXD−HSD interface (*14*). The high acrylamide accessibility of Trp 349 and Trp 775 is reduced upon binding to SecYEG in the absence or presence of ATP, suggesting that SecYEG and the consecutive ATP binding either bring the PPXD and HSD domains closer together or that these domains independently bind or penetrate the SecYEG channel.

Our data clearly demonstrate that the PPXD (Trp 349), NBF-II (Trp 519 and Trp 541), and HWD (Trp 701 and Trp 723) undergo conformational changes upon ATP binding to the SecYEG-bound SecA. Because these changes in acrylamide accessibility of these residues were not observed for the soluble SecA, it can be concluded that the SecYEG-bound SecA adopts an unique conformation that differs from the soluble enzyme. Importantly, this emphasizes the necessity to study the SecYEG-bound SecA more extensively. Currently, most studies on the molecular mechanism of the SecA motor protein are restricted to the soluble enzyme. Our study was performed with single mutants of the endogenous tryptophan positions of SecA. The tryptophanless SecA can now be used to introduce tryptophans at selected positions, and this will make an even more powerful approach in studying the catalytic mechanism of this remarkable motor protein.

ACKNOWLEDGMENT

We thank Nico Nouwen for critically reading of the manuscript.

REFERENCES

1. Hartl, F. U., Lecker, S., Schiebel, E., Hendrick, J. P., and Wickner, W. (1990) The binding cascade of SecB to SecA to SecY/E mediates preprotein targeting to the *E. coli* plasma membrane, *Cell 63*, 269−279.
2. Lill, R., Dowhan, W., and Wickner, W. (1990) The ATPase activity of SecA is regulated by acidic phospholipids, SecY, and the leader and mature domains of precursor proteins, *Cell 60*, 271−280.
3. Ulbrandt, N. D., London, E., and Oliver, D. B. (1992) Deep penetration of a portion of *Escherichia coli* SecA protein into model membranes is promoted by anionic phospholipids and by partial unfolding, *J. Biol. Chem. 267*, 15184−15192.
4. Cabelli, R. J., Dolan, K. M., Qian, L. P., and Oliver, D. B. (1991) Characterization of membrane-associated and soluble states of SecA protein from wild-type and *SecA51(TS)* mutant strains of *Escherichia coli*, *J. Biol. Chem. 266*, 24420−24427.
5. van der Does, C., den Blaauwen, T., de Wit, J. G., Manting, E. H., Groot, N. A., Fekkes, P., and Driessen, A. J. M. (1996) SecA is an intrinsic subunit of the *Escherichia coli* preprotein translocase and exposes its carboxyl terminus to the periplasm, *Mol. Microbiol. 22*, 619−629.

6. Manting, E. H., and Driessen, A. J. M. (2000) *Escherichia coli* translocase: The unravelling of a molecular machine, *Mol. Microbiol. 37*, 226−238.
7. Driessen, A. J. M., Manting, E. H., and van der Does, C. (2001) The structural basis of protein targeting and translocation in bacteria, *Nat. Struct. Biol. 8*, 492−498.
8. de Keyzer, J., van der Does, C., and Driessen, A. J. M. (2003) The bacterial translocase: A dynamic protein channel complex, *Cell Mol. Life Sci. 60*, 2034−2052.
9. Clemons, W. M., Jr., Menetret, J. F., Akey, C. W., and Rapoport, T. (1904) Structural insight into the protein translocation channel, *Curr. Opin. Struct. Biol. 14*, 390−396.
10. Economou, A., and Wickner, W. (1994) SecA promotes preprotein translocation by undergoing ATP-driven cycles of membrane insertion and deinsertion, *Cell 78*, 835−843.
11. Schiebel, E., Driessen, A. J. M., Hartl, F. U., and Wickner, W. (1991) Delta mu H+ and ATP function at different steps of the catalytic cycle of preprotein translocase, *Cell 64*, 927−939.
12. van der Wolk, J. P., de Wit, J. G., and Driessen, A. J. M. (1997) The catalytic cycle of the *Escherichia coli* SecA ATPase comprises two distinct preprotein translocation events, *EMBO J. 16*, 7297−7304.
13. Hunt, J. F., Weinkauf, S., Henry, L., Fak, J. J., McNicholas, P., Oliver, D. B., and Deisenhofer, J. (2002) Nucleotide control of interdomain interactions in the conformational reaction cycle of SecA, *Science 297*, 2018−2026.
14. Osborne, A. R., Clemons, W. M., Jr., and Rapoport, T. A. (2004) A large conformational change of the translocation ATPase SecA, *Proc. Natl. Acad. Sci. U.S.A. 101*, 10937−10942.
15. Sharma, V., Arockiasamy, A., Ronning, D. R., Savva, C. G., Holzenburg, A., Braunstein, M., Jacobs, W. R., Jr., and Sacchettini, J. C. (2003) Crystal structure of *Mycobacterium tuberculosis* SecA, a preprotein translocating ATPase, *Proc. Natl. Acad. Sci. U.S.A. 100*, 2243−2248.
16. Kimura, E., Akita, M., Matsuyama, S., and Mizushima, S. (1991) Determination of a region in SecA that interacts with presecretory proteins in *Escherichia coli*, *J. Biol. Chem. 266*, 6600−6606.
17. Mitchell, C., and Oliver, D. (1993) Two distinct ATP-binding domains are needed to promote protein export by *Escherichia coli* SecA ATPase, *Mol. Microbiol. 10*, 483−497.
18. van der Wolk, J. P., Boorsma, A., Knoche, M., Schafer, H. J., and Driessen, A. J. M. (1997) The low-affinity ATP binding site of the *Escherichia coli* SecA dimer is localized at the subunit interface, *Biochemistry 36*, 14924−14929.
19. Karamanou, S., Vrontou, E., Sianidis, G., Baud, C., Roos, T., Kuhn, A., Politou, A. S., and Economou, A. (1999) A molecular switch in SecA protein couples ATP hydrolysis to protein translocation, *Mol. Microbiol. 34*, 1133−1145.
20. Dapic, V., and Oliver, D. (2000) Distinct membrane binding properties of N- and C-terminal domains of *Escherichia coli* SecA ATPase, *J. Biol. Chem. 275*, 25000−25007.
21. Sianidis, G., Karamanou, S., Vrontou, E., Boulias, K., Repanas, K., Kyrpides, N., Politou, A. S., and Economou, A. (2001) Cross-talk between catalytic and regulatory elements in a DEAD motor domain is essential for SecA function, *EMBO J. 20*, 961−970.
22. van der Wolk, J. P., Klose, M., Breukink, E., Demel, R. A., de Kruijff, B., Freudl, R., and Driessen, A. J. M. (1993) Characterization of a *Bacillus subtilis* SecA mutant protein deficient in translocation ATPase and release from the membrane, *Mol. Microbiol. 8*, 31−42.
23. Rajapandi, T., and Oliver, D. (1996) Integration of SecA protein into the *Escherichia coli* inner membrane is regulated by its amino-terminal ATP-binding domain, *Mol. Microbiol. 20*, 43−51.
24. Breukink, E., Keller, R. C., and de Kruijff, B. (1993) Nucleotide and negatively charged lipid-dependent vesicle aggregation caused by SecA. Evidence that SecA contains two lipid-binding sites, *FEBS Lett. 331*, 19−24.
25. de Keyzer, J., van der Does, C., Kloosterman, T. G., and Driessen, A. J. M. (2003) Direct demonstration of ATP-dependent release of SecA from a translocating preprotein by surface plasmon resonance, *J. Biol. Chem. 278*, 29581−29586.
26. Song, M., and Kim, H. (1997) Stability and solvent accessibility of SecA protein of *Escherichia coli*, *J. Biochem. 122*, 1010−1018.
27. Economou, A., Pogliano, J. A., Beckwith, J., Oliver, D. B., and Wickner, W. (1995) SecA membrane cycling at SecYEG is driven by distinct ATP binding and hydrolysis events and is regulated by SecD and SecF, *Cell 83*, 1171−1181.
28. Vrontou, E., Karamanou, S., Baud, C., Sianidis, G., and Economou, A. (2004) Global coordination of protein translocation by the SecA IRA1 switch, *J. Biol. Chem.*
29. Fekkes, P., de Wit, J. G., Boorsma, A., Friesen, R. H., and Driessen, A. J. M. (1999) Zinc stabilizes the SecB binding site of SecA, *Biochemistry 38*, 5111−5116.
30. Ding, H., Hunt, J. F., Mukerji, I., and Oliver, D. (2003) *Bacillus subtilis* SecA ATPase exists as an antiparallel dimer in solution, *Biochemistry 42*, 8729−8738.
31. van den Berg, B., Clemons, W. M., Collinson, I., Modis, Y., Hartmann, E., Harrison, S. C., and Rapoport, T. A. (2004) X-ray structure of a protein-conducting channel, *Nature 427*, 36−44.
32. Breyton, C., Haase, W., Rapoport, T. A., Kuhlbrandt, W., and Collinson, I. (2002) Three-dimensional structure of the bacterial protein−translocation complex SecYEG, *Nature 418*, 662−665.
33. Manting, E. H., van der Does, C., Remigy, H., Engel, A., and Driessen, A. J. M. (2000) SecYEG assembles into a tetramer to form the active protein translocation channel, *EMBO J. 19*, 852−861.
34. Wang, H. W., Chen, Y., Yang, H., Chen, X., Duan, M. X., Tai, P. C., and Sui, S. F. (2003) Ring-like pore structures of SecA: Implication for bacterial protein-conducting channels, *Proc. Natl. Acad. Sci. U.S.A. 100*, 4221−4226.
35. Yahr, T. L., and Wickner, W. T. (2000) Evaluating the oligomeric state of SecYEG in preprotein translocase, *EMBO J. 19*, 4393−4401.
36. Duong, F. (2003) Binding, activation, and dissociation of the dimeric SecA ATPase at the dimeric SecYEG translocase, *EMBO J. 22*, 4375−4384.
37. Tziatzios, C., Schubert, D., Lotz, M., Gundogan, D., Betz, H., Schagger, H., Haase, W., Duong, F., and Collinson, I. (2004) The bacterial protein−translocation complex: SecYEG dimers associate with one or two SecA molecules, *J. Mol. Biol. 340*, 513−524.
38. Natale, P., Swaving, J., van Der, D. C., de Keyzer, J., and Driessen, A. J. M. (2004) Binding of SecA to the SecYEG complex accelerates the rate of nucleotide exchange on SecA, *J. Biol. Chem. 279*, 13769−13777.
39. Schmidt, M. G., Rollo, E. E., Grodberg, J., and Oliver, D. B. (1988) Nucleotide sequence of the *secA* gene and *secA(Ts)* mutations preventing protein export in *Escherichia coli*, *J. Bacteriol. 170*, 3404−3414.
40. Fak, J. J., Itkin, A., Ciobanu, D. D., Lin, E. C., Song, X. J., Chou, Y. T., Gierasch, L. M., and Hunt, J. F. (2004) Nucleotide exchange from the high-affinity ATP-binding site in SecA is the rate-limiting step in the ATPase cycle of the soluble enzyme and occurs through a specialized conformational state, *Biochemistry 43*, 7307−7327.
41. den Blaauwen, T., Fekkes, P., de Wit, J. G., Kuiper, W., and Driessen, A. J. M. (1996) Domain interactions of the peripheral preprotein translocase subunit SecA, *Biochemistry 35*, 11994−12004.
42. Kourtz, L., and Oliver, D. (2000) Tyr-326 plays a critical role in controlling SecA-preprotein interaction, *Mol. Microbiol. 37*, 1342−1356.
43. Ding, H., Mukerji, I., and Oliver, D. (2001) Lipid and signal peptide-induced conformational changes within the C-domain of *Escherichia coli* SecA protein, *Biochemistry 40*, 1835−1843.
44. Weaver, A. J. M., McDowall, A. W., Oliver, D. B., and Deisenhofer, J. (1992) Electron microscopy of thin-sectioned three-dimensional crystals of SecA protein from *Escherichia coli*: Structure in projection at 40 Å resolution, *J. Struct. Biol. 109*, 87−96.
45. Song, W., Raden, D., Mandon, E. C., and Gilmore, R. (2000) Role of Sec61α in the regulated transfer of the ribosome-nascent chain complex from the signal recognition particle to the translocation channel, *Cell 100*, 333−343.
46. Sambrook, J., Fritsch, E. F., and Maniatis, T. (1989) *Molecular Cloning: A Laboratory Manual*, 2nd ed., Cold Spring Habor Laboratory Press, Cold Spring Habor, New York.
47. Yanisch-Perron, C., Vieira, J., and Messing, J. (1985) Improved M13 phage cloning vectors and host strains: Nucleotide sequences of the M13mp18 and pUC19 vectors, *Gene 33*, 103−119.
48. Oliver, D. B., and Beckwith, J. (1982) Regulation of a membrane component required for protein secretion in *Escherichia coli*, *Cell 30*, 311−319.

49. Klose, M., Schimz, K. L., van der Wolk, J., Driessen, A. J. M., and Freudl, R. (1993) Lysine 106 of the putative catalytic ATP-binding site of the *Bacillus subtilis* SecA protein is required for functional complementation of *Escherichia coli secA* mutants *in vivo*, *J. Biol. Chem. 268*, 4504−4510.
50. Or, E., Navon, A., and Rapoport, T. (2002) Dissociation of the dimeric SecA ATPase during protein translocation across the bacterial membrane, *EMBO J. 21*, 4470−4479.
51. Lakowicz, J. R. (1999) *Principles of Fluorescence Spectroscopy*, 2nd ed., Kluwer Academic/Plenum Publishers, New York.
52. de Keyzer, J., van der Does, C., and Driessen, A. J. M. (2002) Kinetic analysis of the translocation of fluorescent precursor proteins into *Escherichia coli* membrane vesicles, *J. Biol. Chem. 277*, 46059−46065.
53. Guex, N., and Peitsch, M. C. (1997) SWISS-MODEL and the Swiss-PdbViewer: An environment for comparative protein modeling, *Electrophoresis 18*, 2714−2723.
54. Burstein, E. A. (1976) Luminescence of protein chromophores. Model Studies, in *Advances in Science and Technology (Itogi Nauki i Tekhniki)* 6th ed., VINITI, Moscow, Russia.
55. Ramamurthy, V., and Oliver, D. (1997) Topology of the integral membrane form of *Escherichia coli* SecA protein reveals multiple periplasmically exposed regions and modulation by ATP binding, *J. Biol. Chem. 272*, 23239−23246.
56. van der Does, C., Manting, E. H., Kaufmann, A., Lutz, M., and Driessen, A. J. M. (1998) Interaction between SecA and SecYEG in micellar solution and formation of the membrane-inserted state, *Biochemistry 37*, 201−210.
57. Eichler, J., and Wickner, W. (1997) Both an N-terminal 65-kDa domain and a C-terminal 30-kDa domain of SecA cycle into the membrane at SecYEG during translocation, *Proc. Natl. Acad. Sci. U.S.A. 94*, 5574−5581.

BI047488R